Detection of Tamarisk Defoliation by the Northern Tamarisk Beetle Based on Multitemporal Landsat 5 Thematic Mapper Imagery

Ran Meng[1] and Philip E. Dennison
Department of Geography, University of Utah,
260 S. Central Campus Drive, Room 270,
Salt Lake City, Utah 84112

Levi R. Jamison
School of Natural Resources and the Environment,
1110 E. South Campus Drive, Room 123- Building #33,
University of Arizona, Tucson, Arizona 85721-0033

Charles van Riper III and Pamela Nagler
U.S. Geological Survey, Southwest Biological Science Center,
Sonoran Desert Research Station, Tucson, Azrizona 85719

Kevin R. Hultine
Desert Botanical Garden, 1201 N. Galvin Parkway,
Phoenix, Arizona 85008

Dan W. Bean
Biological Pest Control, Colorado Department of Agriculture,
750 37.8 Road, Palisade, Colorado 81526-9740

Tom Dudley
Marine Science Institute, University of California, Santa Barbara,
Santa Barbara California 93106-6150

Abstract: The spread of tamarisk (*Tamarix* spp., also known as saltcedar) is a significant ecological disturbance in western North America and has long been targeted for control, leading to the importation of the northern tamarisk beetle (*Diorhabda carinulata*) as a biological control agent. Following its initial release along the Colorado River near Moab, Utah in 2004, the beetle has successfully established and defoliated tamarisk across much of the upper Colorado River Basin. However, the spatial distribution and seasonal timing of defoliation are complex and difficult to quantify over large areas. To address this challenge, we tested and compared two remote sensing approaches to mapping tamarisk defoliation: Disturbance Index (DI) and a

[1]Corresponding author; email: Ran.Meng@utah.edu

GIScience & Remote Sensing, 2012, **49**, No. 4, p. 510–537. http://dx.doi.org/10.2747/1548-1603.49.4.510

decision tree method called Random Forest (RF). Based on multitemporal Landsat 5 TM imagery for 2006–2010, changes in DI and defoliation probability from RF were calculated to detect tamarisk defoliation along the banks of Green, Colorado, Dolores and San Juan rivers within the Colorado Plateau area. Defoliation mapping accuracy was assessed based on field surveys partitioned into 10 km sections of river and on regions of interest created for continuous riparian vegetation. The DI method detected 3711 ha of defoliated area in 2007, 7350 ha in 2008, 10,457 ha in 2009 and 5898 ha in 2010. The RF method detected much smaller areas of defoliation but proved to have higher accuracy, as demonstrated by accuracy assessment and sensitivity analysis, with 784 ha in 2007, 960 ha in 2008, 934 ha in 2009, and 1008 ha in 2010. Results indicate that remote sensing approaches are likely to be useful for studying spatiotemporal patterns of tamarisk defoliation as the tamarisk leaf beetle spreads throughout the western United States.

INTRODUCTION

Since its introduction from Asia in the early 1800s, tamarisk (*Tamarix* spp., a.k.a. saltcedar) has gradually become one of the most widely dispersed invasive, natural community–altering trees/shrubs in the western United States (Barrows, 1996; Friedman et al., 2005; Shafroth et al., 2005). Tamarisk is relatively drought tolerant and can displace or replace native riparian vegetation, such as cottonwood and willow (Warren and Turner, 1975; Busch and Smith, 1995; Cleverly et al., 1997; Lesica and Miles, 2004). Previous work has estimated that tamarisk occupies 526,000 hectares of the western United States (Bailey et al.,2001).

Impacts of tamarisk invasion include reduced biodiversity, increases in soil surface salinity, changes in riparian wildfire occurrence, and concerns regarding increased water use (Johns, 1989; Dudley et al., 2000; Shafroth et al., 2005). Tamarisk has been ranked as one of the ten worst noxious weeds in the United States because of its cumulative effects (Lesica and Miles, 2004). Tamarisk costs the western United States between $133 and $185 million annually according to an economic assessment of ecosystem services lost (Brown et al., 1989; Zavaleta, 2000). Thus, tamarisk is viewed as a significant ecological threat and has been targeted for control in recent decades. Conventional control methods for tamarisk involve chemical and mechanical treatments, sometimes in combination with fire prescription (Harms and Hiebert, 2006), all of which can result in collateral damage to other natural resources.

The northern tamarisk beetle, *Diorhabda carinulata*, has been introduced throughout the western United States for the control of tamarisk (DeLoach et al., 2003; Lewis et al., 2003; Shafroth et al. 2005; Tracy and Robbins, 2009). The beetle selectively feeds on tamarisk in both the larval and adult stages. Specifically, the beetle removes the leaf cuticle, causing the leaf to desiccate and drop. Large populations of the beetle can quickly defoliate a tamarisk stand. Tamarisk is not killed by defoliation and can refoliate. Repeated defoliation over several years can result in mortality, although the percentage varies from site to site (Carruthers et al., 2008; Dudley and Bean, 2012). Pupation and adult overwintering take place in litter underneath the tamarisk canopy. Beetles break dormancy and begin feeding on tamarisk several weeks after tamarisk foliage emerges in the spring.

After being released along the Colorado River near Moab, Utah, starting in 2004, the beetles established and defoliated increasingly larger areas of tamarisk as populations expanded. By 2007 beetles had reached high population densities near release sites and then began dispersing away from the release sites and spreading across the Colorado Plateau (Hultine et al., 2010a). Post-release monitoring is a critical element of weed biological control (Blossey, 2004). Since then, multiple ground survey efforts have been used to evaluate tamarisk defoliation (van Riper III et al., 2008; Hultine et al., 2009, 2010b; Moran et al., 2009; Pattison et al., 2011). Field measurements of tamarisk defoliation and mortality are important, but have limited spatial coverage, and are time and labor intensive. Remote sensing has advantages of consistent multispectral and multitemporal data coverage, synoptic observation, and cost effectiveness for study of invasive species (Joshi et al., 2004; Anderson et al., 2005). As the beetle has spread, defoliation has grown to cover an extensive area that is difficult and/or expensive to measure from the ground. Remote sensing provides the only practical way to conduct post-release monitoring at the regional spatial scale needed for evaluation of the tamarisk biocontrol program (Carruthers et al., 2008; Dennison et al., 2009). The goal of this study was to test and compare two remote sensing approaches for mapping tamarisk defoliation caused by the northern tamarisk beetle.

BACKGROUND

Remote Sensing Change Detection

Remote sensing has long been a valuable resource for the detection and study of changes in environment caused by both natural and anthropogenic factors for various purposes (e.g., disturbance damage assessment and monitoring of land cover change) (Singh, 1989 ; Coppin and Bauer, 1996). Two criteria could be used for broadly characterizing change detection: (1) the transformation procedure applied to the data (if any); and (2) analysis techniques used for measuring areas of apparent alteration (Singh, 1989). Multiple approaches have been used to detect changes in land cover, land use, and environmental processes. Commonly used data transformations include principal components analysis (PCA), tasseled-cap (TC) transformation, and change vector analysis (CVA) (Lodwick, 1979; Malila, 1980; Banner and Lynham, 1981; Healey et al., 2005; Jin and Sader, 2005). Analysis techniques such as imaging differencing and ratioing (Wilson et al., 1976; Weismiller et al., 1977), classification routines including supervised and unsupervised methods (Howarth and Wickware, 1981; Bruzzone and Prieto, 2000), regression analysis, and knowledge-based expert systems (Singh, 1989; Wang, 1993) are also employed for change detection. Analysis methods can utilize differences in multitemporal measures or compare independently produced classifications for different dates (Singh, 1989).

Change Detection of Insect-caused Plant Disturbance

Remote sensing can be used for detecting and assessing biophysical changes in plant canopies caused by plant stress (Nilsson, 1995), where stress here means any disturbance that impairs plant health, such as insect outbreak, plant disease, and inadequate water or nutrient supply (Jackson, 1986). Physiological changes occur within plant canopies because of stress. Reduced water supply closes stomata and hinders photosynthesis, causing reduced evapotranspiration (ET) and increased leaf surface temperature (Nilsson, 1995). More severe drought stress, disease, and insect damage can further result in the loss of leaf area.

Different types of remote sensing data and approaches have been used to detect and monitor insect disturbances with varying degrees of success. Landsat 5 Thematic Mapper (TM) and Landsat 7 Enhanced Thematic Mapper (ETM+) imagery has been used to identify forest defoliation caused by gypsy moth caterpillars in Ohio and southern Siberia (Kharuk et al., 2003; Hurley et al., 2004). Hurley et al. (2004) assessed defoliation by gypsy moth caterpillars using a haze-adjusted ratio of TM spectral band 4 (near-infrared) to TM spectral band 3 (visible red). The ratio values between two dates were subtracted in order to identify defoliation. Ratio subtraction values were further analyzed using CVA to more effectively isolate areas where defoliation occurred (Hurley et al., 2004). Multitemporal Landsat 7 ETM+ imagery was used to study tree mortality caused by mountain pine beetle in the Prince George Forest Region of British Columbia (Skakun et al., 2003). In that study, an Enhanced Wetness Difference Index (EWDI) was calculated to interpret spectral patterns in stands with the "red attack" stage of tree mortality. High spatial resolution QuickBird multispectral imagery has also been used to detect mountain pine beetle mortality (Coops et al., 2006). The Red-Green Index (RGI), a ratio of red reflectance to green reflectance, was most successful at separating undamaged tree crowns from red crowns (Coops et al., 2006).

In the central part of the Šumava Mountains in Central Europe, multitemporal Landsat TM/ETM+ imagery combined with field vegetation data was used to study two types of disturbances of spruce forest: bark beetle outbreak and clear-cuts (Hais et al., 2009). Hais et al. (2009) used the following spectral indices for disturbance detection: Normalized Difference Moisture Index (NDMI), Disturbance Index (DI), Tasseled Cap (TC) transformation bands, and Modified Disturbance Index (DI′). DI, wetness, greenness, and brightness indices showed the highest sensitivity to forest disturbance for both disturbance types. DeRose et al. (2011) studied the death of Engelmann spruce (*Picea engelmannii*) by spruce beetle in southern Utah using multitemporal Landsat 5 TM imagery. Change in DI value for each image was calculated to classify the imagery (DeRose et al., 2011).

METHODS

Study Area

The study area was defined by the combined area of three Landsat 5 TM scenes (path 36, row 32; path 36, row 33; path 36, row 34). The area covered by the three scenes includes eastern Utah and western Colorado (Fig. 1). In the study area, the Colorado River flows from northeast to southwest before entering Lake Powell. Near the Colorado/Utah state boundary the Dolores River enters the Colorado River. Further downstream, the Green River also intersects the Colorado River roughly 50 km upstream of Lake Powell. Another major tributary, the San Juan River in the southern part of study area, flows from east to west and joins the Colorado River at Lake Powell.

Dominant native riparian tree species within the study area include Fremont cottonwood (*Populus fremontii*), box elder (*Acer negundo*), New Mexican privit

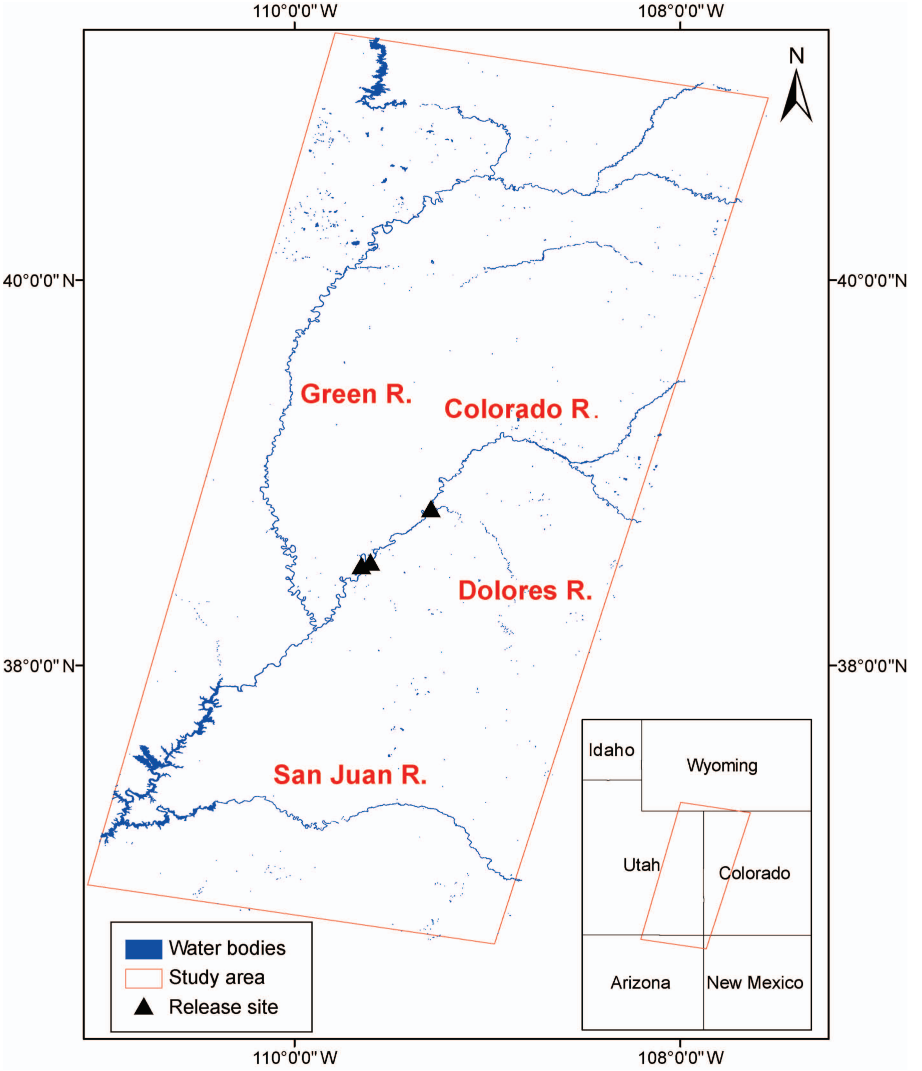

Fig. 1. The study area, encompassing eastern Utah and western Colorado, and release sites of the northern tamarisk beetle in 2004.

(*Forestiera neomexicana*), and two willow species (*Salix exigua* and *S. goodingi*). However, tamarisk has extensively replaced native riparian vegetation species along the stream banks and formed dense stands in much of the study area. In 2004 northern tamarisk beetle adults were first released within the study area and became well established at three locations along the Colorado River; one near the confluence of the Colorado and Dolores rivers and at two locations downstream of Moab, Utah. In 2007 beetle adults were also established along the San Juan River in Bluff, Utah. Beginning in 2007, the beetle rapidly spread within the study area and has resulted in substantial defoliation of tamarisk stands.

Table 1. Dates and Estimated Cloud Cover for Each Scene Used in the Study

Path	Row	Dates	Estimated cloud cover (%)
36	32	27 Aug 2006	10
36	32	30 Aug 2007	0
36	32	15 Jul 2008	2
36	32	19 Aug 2009	0
36	32	06 Aug 2010	11
36	33	27 Aug 2006	0
36	33	30 Aug 2007	0
36	33	15 Jul 2008	2
36	33	04 Sep 2009	10
36	33	19 Aug 2009	0
36	33	06 Aug 2010	4
36	34	27 Aug 2006	0
36	34	30 Aug 2007	0
36	34	15 Jul 2008	4
36	34	04 Sep 2009	8
36	34	19 Aug 2009	0
36	34	06 Aug 2010	1

Image Processing

Annual Landsat 5 TM images covering 2006–2010 were obtained from the USGS GLOVIS website (http://glovis.usgs.gov). Anniversary dates in late August and early September were targeted to capture defoliation near its peak in expansion during the active summer season, but before major refoliation in the weeks following beetle defoliation. If low–cloud cover images were not available in the targeted date range, an earlier date was used. Dates for all scenes used in image processing are listed in Table 1. Due to shifts in the exact spatial coverage of each TM scene, a mask containing the area common to all years was used to restrict the study area. ACORN (Atmosphere CORrection Now; http://www.imspec.com) was used to carry out atmosphere correction to apparent surface reflectance for the 19 August 2009 scene in each path-row due to low cloud cover. All other dates were then intercalibrated using pseudo-invariant pixels found by iMAD (Iteratively re-weighted Multivariate Alteration Detection; Canty and Nielsen, 2008). As a radiometric normalization method, iMAD can be easily implemented for both multi- and hyperspectral imagery automatically (Canty and Nielsen, 2008). Masks of cloud and cloud shadows for multitemporal TM images were generated using the algorithm used by Kennedy et al. (2010), and then applied to the images. After the calculation of a cloud score and shadow score for each image

Table 2. Threshold of DI Change for Each Image[a]

Path, row	2007	2008	2009	2010
Path 36, Row 32	0.15	0.11	0.11	0.11
Path 36, Row 33	0.11	0.11	0.11	0.11
Path 36, Row 34	0.11	0.14	0.11	0.11

[a]If the change in DI within a pixel was greater than or equal to the value listed in the table, the pixel was classified as defoliated. An additional threshold, used for masking cloud effects, is not shown.

based on three TC components (brightness, greenness, and wetness), the thresholds of score images were determined for each year through visual inspection of the images (Kennedy et al., 2010).

Disturbance Index (DI). The DI algorithm for forest disturbance detection developed by Healey et al. (2005) was the first measure used to detect changes in tamarisk canopy cover likely caused by beetle defoliation. As a first step, the TC transformation was calculated for all intercalibrated images. The TC transformation reduced six TM bands (excluding the thermal band) to three component bands: brightness, greenness, and wetness (Crist and Cicone, 1984). Unlike Healey et al. (2005), the three TC bands were not normalized because the images had already been intercalibrated. DI was calculated directly as:

$$\mathrm{DI} = \mathrm{Brightness} - (\mathrm{Greenness} + \mathrm{Wetness})\,. \tag{1}$$

A disturbed area decreasing in vegetation cover would have lower greenness and wetness values, and could be accompanied by an increase in brightness due to exposed soil (Healey et al., 2005). Change in DI was calculated by subtracting the DI values for each image from the DI values of a baseline image. The 2006 images were used as the baseline, assuming that defoliation within the study area during this time frame was negligible. DI values higher than the baseline DI value indicate a loss of vegetation cover, and DI values lower than the baseline DI value indicate an increase in vegetation cover.

DI change images for each year were manually compared against an RGB combination of TM bands 4, 3, and 2 to find a threshold in DI change that indicated tamarisk defoliation. Based on the visual inspection, the DI change threshold used to detect defoliation was assigned independently for each image (Table 2), with the goal of detecting apparently defoliated pixels while excluding apparently non-defoliated pixels at the same time. Change in DI was found to detect changes in both riparian and non-riparian vegetation, so National Land Cover Dataset (NLCD; http://landcover.usgs.gov/landcoverdata.php) class 90 (Woody Wetland) was used to select areas of riparian vegetation likely to contain tamarisk. All other classes were masked out of the DI change analysis. Residual cloud effects can have high DI values, so a maximum change in DI was also set for each image.

Random Forest (RF). The second algorithm used to map defoliation was Random Forest (RF; Liaw and Wiener, 2002), developed by Breiman (2001). RF improves on

Table 3. Threshold of RF Probability for Each Image[a]

Path, row	2007	2008	2009	2010
Path 36, Row 32	0.60	0.60	0.50	0.60
Path 36, Row 33	0.95	0.80	0.90	0.90
Path 36, Row 34	0.80	0.80	0.80	0.70

[a]If the RF probability within a pixel was greater than or equal to the value listed in the table, the pixel was classified as defoliated.

the traditional decision tree classification (Pal and Mather, 2003) by selecting variables at random out of a large number of input variables without deletion of split nodes, resulting in a large, random ensemble of independent tree classifiers that vote for class membership (Breiman, 2001). This method is able to overcome the over-fitting drawback of traditional decision tree classifiers and selects the most useful variables for classifying features from inputs (Breiman, 2001). As a first step, a suite of variables was calculated for each intercalibrated image. These variables included homogeneity of co-occurrence texture measures, TC transformation bands (brightness, greenness, and wetness), and PCA bands. TC components have been successfully used for vegetation disturbance detection (Healey et al. 2005); PCA transformation is a commonly used method for change detection (Lodwick, 1979); texture information has long been used for classification and change detection (Smith et al., 2002). A total of 42 variables calculated for the target year and 2006 baseline year were used as inputs for RF. A training dataset containing defoliated and non-defoliated pixels was created using visual inspection of the TM images. Based on the training data, 500 independent decision trees were used to calculate the probability that each pixel belonged to the defoliated class. Training was done just for the 2006–2007 date pair, and then applied to all years. RF produced a probability of belonging to the defoliated class for each year (2007–2010). Because probability is a continuous measure, probability images were converted to maps of defoliation using a threshold determined by manual comparison with a 4, 3, 2 (RGB) TM image, in the same way as when using the DI method (above). The probability threshold was determined independently for each image (Table 3). Similar to the DI method, NLCD class 90 (Woody Wetland) was used to select areas of riparian vegetation likely to contain tamarisk.

Ground Truth Data Collection

Ground surveys of northern tamarisk beetle presence and tamarisk defoliation were conducted within the study area in 2007–2010. Observations were recorded at points spaced 1.5 km apart within the riparian zone along the Colorado, Green, Dolores, and San Juan rivers and at randomly spaced areas in between. The San Juan River was only surveyed in 2009 and 2010. At each point, estimates of defoliation status were made for tamarisk within a 100 m radius of the point. Classes of high (67–100%), medium (34–66%), low (1–33%), or absent (0%) defoliation were used, except in 2010 when continuous defoliation percentages were estimated for the 100 m radius surrounding each point. Points were used for accuracy assessment if their collection date fell within a time window spanning one week prior to or two weeks following image acquisition.

Table 4. Percentage of Woody Wetland Area Within Different Distance Buffers of Streams in the Study Area

Buffer distance (m)	Percent of Woody Wetland area
100	69
200	82
300	89
400	92
500	94
1000	99

The selected set of points included 317 points in 2007, 370 points in 2008, 275 points in 2009, and 342 field points in 2010.

Accuracy Assessment

Two methods were used to assess the accuracy of defoliation detection using DI and RF. Field data were grouped by 10 km river sections and compared to defoliation detections within each section. Accuracy was also assessed using manually assigned regions of interest (ROIs).

For the river section method, we divided each major river within the study area into 10 km sections. The NLCD Woody Wetland class was used to create a buffer distance from a streams dataset provided by the Utah Automated Geographic Reference Center (http://gis.utah.gov). Analysis showed that 94% of the Woody Wetland class area was within a 500 m buffer of streams in the study area (Table 4). Using this 500 m distance, each 10 km river section was buffered to include the riparian zone along each river. As a result, 380 sections, each with a unique identifier, were created within the study area. Field data points falling within a section buffer were assigned to that section. If any point within a section had recorded defoliation, the section was labeled as defoliated (Figure 2). If no points within a section had recorded defoliation, the section was labeled as non-defoliated. A zonal function was used to count all pixels with DI change and RF defoliation probability exceeding the set thresholds within each section. Error matrices were used to compare defoliation detection by DI and RF to defoliation detection by field survey across all river sections. Kappa coefficients for each year were also calculated based on the error matrices. Unlike overall accuracy, kappa takes into account agreement by chance (Cohen, 1960).

The ROI accuracy assessment method involved use of a false color infrared (4, 3, 2) band combination, in which healthy vegetation appears scarlet in color while defoliated pixels of tamarisk appeared black, brown, or grey in color. ROIs of apparent defoliated and non-defoliated riparian vegetation were drawn manually by visual interpretation of the 4, 3, 2 image display. For the ROIs of non-defoliated and defoliated areas, a random sample of 20 percent of the pixels within all ROI polygons for each year was used for accuracy assessment (Table 5). Defoliation detections using DI and RF were then compared to the randomly selected pixels using error matrices. Kappa coefficients for each year were also calculated.

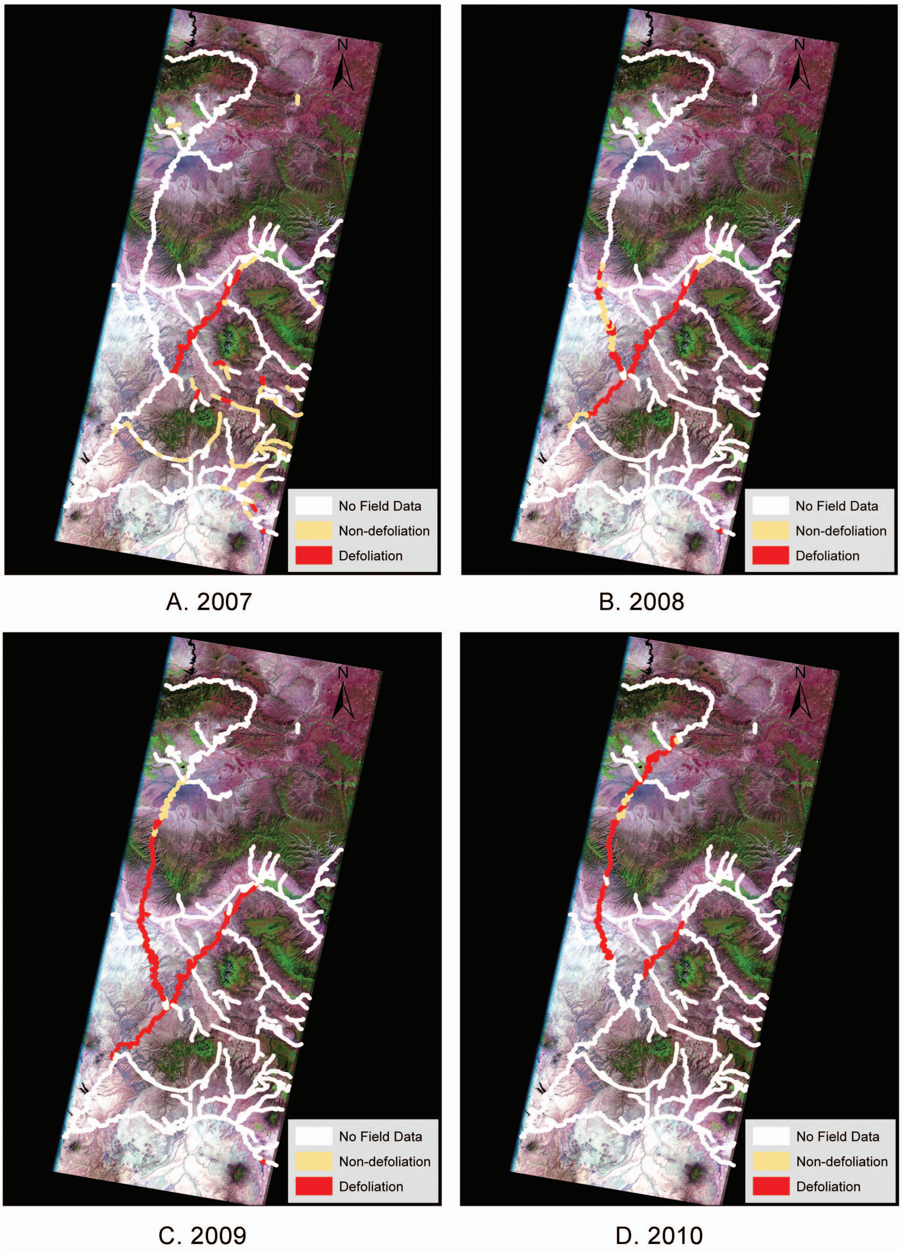

Fig. 2. Tamarisk defoliation field survey data assigned to river sections for 2007–2010.

Sensitivity Analysis

A sensitivity analysis on the thresholds used for both detection methods was implemented with Receiver Operating Characteristic (ROC) curves in ENVI 4.7 (http://www.exelisvis.com/) using ROIs drawn in the preceding section. ROC curves

Table 5. Number of Sample Points for 2007–2010

Year	Total defoliation pixels	Total non-defoliation pixels
2007	1357	1412
2008	1319	1376
2009	1462	1499
2010	1317	1330

can compare detection results with continuous threshold values to ground-truth information, in order to evaluate the performance and sensitivity of a classifier and select the proper threshold (Bradley, 1997). In addition, the sensitivity of kappa to increasing the number of pixels in each river section necessary to classify a section as defoliated was examined for both detection methods (DI and RF).

RESULTS

The TM time series captured the spatiotemporal patterns of tamarisk defoliation linked with the spread of the northern tamarisk beetle. The number of river sections and the number of pixels in each river section classified as defoliated grew from 2007 to 2009 as the beetle's range expanded (Figs. 3 and 4). In 2007, the most extensive defoliation mostly occurred in the middle portion of the Colorado River and lower Green River. Sections with large numbers of defoliated pixels spread into the middle portion of the Green River and its tributaries in 2008. In 2009 and 2010, the DI method identified defoliation along most of the tributaries in the study area. The RF method was less sensitive, and detected less defoliation within the study area (Fig. 5), especially in the upstream portions of the Colorado River, San Juan River, and Dolores River.

The number of 10 km river sections including defoliation detections also showed a clear pattern of spread. For DI, the pattern started with 221 sections in 2007, increased to 255 in 2008 and 280 in 2009, and finally declined to 251 in 2010. For RF, it started with 136 sections in 2007, fell to 134 in 2008, and then increased to 179 in 2009 and 183 in 2010.

DI Results and Accuracy

Two of the three TC components (greenness and wetness) sharply decreased with defoliation, leading to large positive DI change values (Fig. 6). Brightness demonstrated less change, and many defoliated pixels decreased in brightness due to the exposure of a dark litter layer underneath the tamarisk canopy. As a result of the small reductions in brightness caused by defoliation, changes in wetness and greenness primarily contributed to the detection of defoliation, to a much greater degree than change in brightness.

River section error matrices were used to compare defoliation detected by DI change to defoliation measured in the field (Table 6). In 2007, thresholded DI change found defoliation in only a third of the measured river sections. By 2010, defoliation

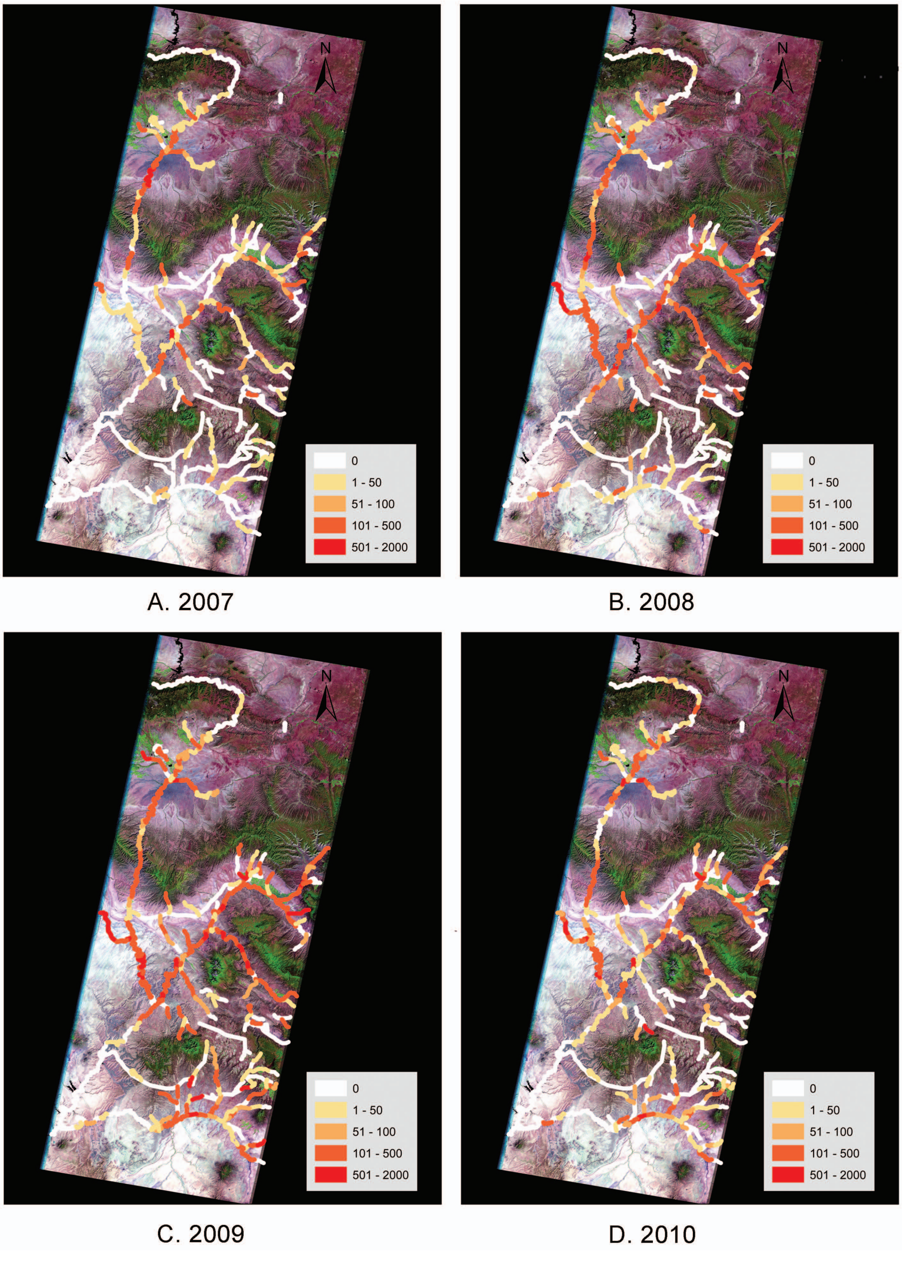

Fig. 3. Number of pixels detected by DI as defoliated in each river section for 2007–2010.

was present at nearly 90% of the measured river sections. However, classification of defoliation using DI change produced multiple false positives in each year. As a result, producer's accuracy values for non-defoliation were very low in 2008, 2009, and 2010 (Table 6). In contrast, the producer's accuracy for defoliation detection always

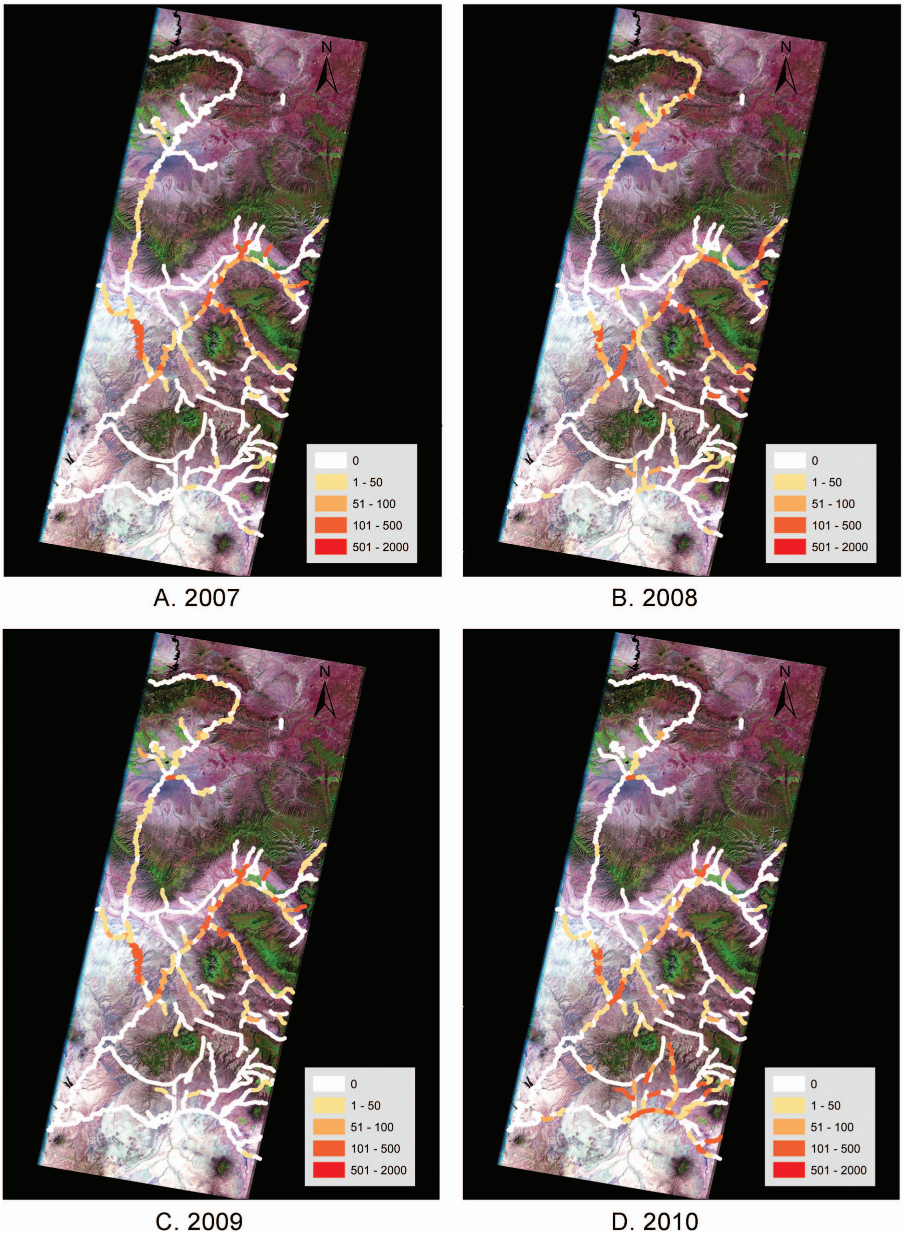

Fig. 4. Number of pixels detected by RF as defoliated in each river section for 2007–2010.

remained high: 2008, 2009, and 2010 values all exceeded 95%. User's accuracy for defoliation ranged from 57.5% to 90%, increasing over the four-year span as the percentage of defoliated sections increased. However, user's accuracy for non-defoliation had the reverse trend, decreasing from 89.74% to 0% over the four-year span. There was an ascending trend in overall accuracy. In 2007, overall accuracy was just 73.10%,

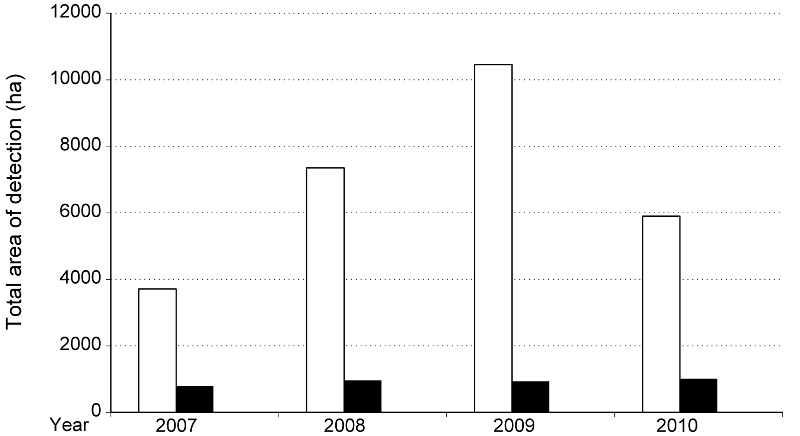

Year	2007	2008	2009	2010
□ DI defoliated area (ha)	3711	7350	10457	5898
■ RF defoliated area (ha)	784	960	934	1008
DI % total Woody Wetland area	1.5	3.59	6.54	3.14

Fig. 5. Total Woody Wetland area mapped as defoliated for 2007–2010, including the percentage of Woody Wetland area within the study area that was mapped as defoliated by the DI method.

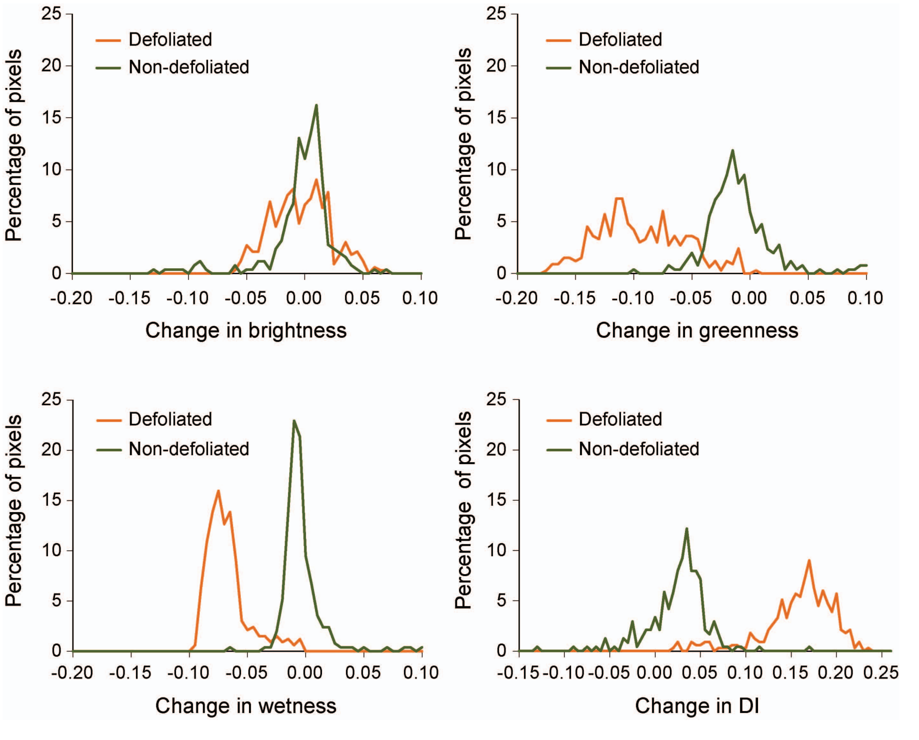

Fig. 6. Distribution of changes in TC components (brightness, greenness, and wetness) and DI between 2006 and 2007 for defoliated and non-defoliated ROI pixels.

Table 6. DI Error Matrices Showing the Number of Defoliated and Non-defoliated River Sections for 2007–2010

	Field-surveyed non-defoliation sections	Field-surveyed defoliation sections	User's accuracy (%)
		2007	
DI non-defoliation sections	35	4	89.74
DI defoliation sections	17	22	57.50
Producer's accuracy (%)	67.31	84.62	
Overall accuracy (%) and kappa	73.10	0.462	
		2008	
DI non-defoliation sections	3	1	75.00
DI defoliation sections	14	37	72.55
Producer's accuracy (%)	17.65	97.37	
Overall accuracy (%) and kappa	72.72	0.190	
		2009	
DI non-defoliation sections	2	2	50.00
DI defoliation sections	9	62	87.32
Producer's accuracy (%)	18.18	96.88	
Overall accuracy (%) and kappa	85.33	0.204	
		2010	
DI non-defoliation sections	0	1	0
DI defoliation sections	5	45	90.00
Producer's accuracy (%)	0	97.83	
Overall accuracy (%) and kappa	88.20	–0.034	

and then decreased slightly to 72.72% in 2008, before increasing to 85.33% in 2009 and 88.20% in 2010. Kappa coefficients were generally low and decreased over time (from 0.462 to –0.034). In 2008–2010, the predominance of field-surveyed defoliated sections resulted in kappa values that were little better than chance occurrence. With choice of an appropriate threshold, the DI method has the potential to successfully distinguish most of the defoliated pixels from non-defoliated ones; however, the tendency of false-positive detection (commission) at the river section scale was inevitable to a certain extent because of the overlapping ranges of change in DI between defoliated and non-defoliated pixels (Fig. 6). Falsely detected defoliation, along with increasing dominance of defoliated river sections within the study area, resulted in declining kappa values over time.

Table 7. DI Error Matrices Showing the Number of Defoliated and Non-defoliated Pixels Classified from ROIs for 2007–2010

	Image interpreted defoliation pixels	Image interpreted non-defoliation pixels	User's accuracy (%)
		2007	
DI defoliation pixels	190	5	97.44
DI non-defoliation pixels	81	277	77.37
Producer's accuracy (%)	70.11	98.23	
Overall accuracy (%) and kappa	84.45	0.687	
		2008	
DI defoliation pixels	128	8	94.12
DI non-defoliation pixels	136	267	66.25
Producer's accuracy (%)	48.48	97.09	
Overall accuracy (%) and kappa	73.28	0.46	
		2009	
DI defoliation pixels	160	13	92.49
DI non-defoliation pixels	132	287	68.5
Producer's accuracy (%)	54.79	95.67	
Overall accuracy (%) and kappa	75.51	0.507	
		2010	
DI defoliation pixels	172	0	100
DI non-defoliation pixels	91	266	74.51
Producer's accuracy (%)	65.4	100	
Overall accuracy (%) and kappa	82.8	0.655	

The error matrix for the ROI-based accuracy assessment, which was less sensitive to false detection than the river section–based method, suggested little change in defoliation classification accuracy from 2007 to 2010 (Table 7). The year 2007 had the highest overall accuracy (84.45%) and kappa coefficient (0.687), while 2008 had the lowest accuracy with the overall accuracy and the kappa coefficient decreasing to 73.28% and 0.460, respectively. Producer's accuracy for non-defoliation was always higher than for defoliation, and user's accuracy for defoliation was always higher than for non-defoliation. This suggests that the detections of defoliation at the pixel-level tended toward omission.

Table 8. Variables That Reduced Classification Error Rate More than 50% for 2007 Defoliation Classification Using Random Forest

Variable	Decrease in error rate (%)
2007 Thematic Mapper Band 4	78.39
2006 Principal Components Band 3	71.35
2007 Principal Components Band 3	66.45
2007 Tasseled-Cap Band Greenness	66.38
2006 Tasseled-Cap Band Greenness	65.64
2006 Thematic Mapper Band 1	62.23
2006 Homogeneity of Co-occurrence Texture Measures Band 7	57.85
2007 Tasseled-Cap Band Brightness	57.06
2007 Thematic Mapper Band 1	55.96
2007 Principal Components Analysis Band 1	55.84
2007 Thematic Mapper Band 2	55.52
2006 Thematic Mapper Band 4	51.11

RF Results and Accuracy

The RF method automatically selected the variables that most decreased classification error from 42 input bands. The variables that resulted in the largest decreases in error rate reveal the variables that are important for separating defoliated from non-defoliated pixels. Table 8 shows variables ranked in order of importance for the tamarisk defoliation classification based on the 2006–2007 pair. The most important variable was TM band 4 (near infrared) from 2006, likely due to healthy tamarisk having a high band 4 reflectance in the baseline year. Principal component bands for 2006 and 2007 had the second and third largest effects on the classification for reducing classification error. In addition, homogeneity of co-occurrence texture measures also helped to reduce classification error. Greenness and brightness TC components, from which DI was calculated, were included in the list of variables in Table 8.

River section and ROI-based error matrices were used to evaluate the accuracy of defoliation detected by the RF method. Compared with the DI change method, RF produced fewer false positives in each year, but failed to detect defoliation in some river sections (Table 9). As a result, producer's accuracy values for non-defoliation were much higher compared to DI over the four-year span: 88.46% in 2007, 69.57 % in 2008, 64.71% in 2009, and 86.67 % in 2010. Producer's accuracy values for defoliation were relatively high except in 2010: 84.62% in 2007, 76.32% in 2008, 82.81% in 2009, and 56.52% in 2010. The user's accuracy for defoliation also remained relatively high over the entire four-year span, with user's accuracy for defoliation exceeding 80% in three years. However, user's accuracy for non-defoliation decreased over the four-year span as the percentage of defoliated river sections increased. There was a descending trend in overall accuracy. In 2007, the overall accuracy was 87.20%, and subsequently decreased to 63.90% in 2010. Although kappa coefficients exhibited a decreasing trend over time, kappa values for RF were higher than those for DI.

Table 9. RF Error Matrices Showing the Number of Defoliated and Non-defoliated River Sections for 2007–2010

	Field-surveyed non-defoliation sections	Field-surveyed defoliation sections	User's accuracy (%)
		2007	
RF non-defoliation sections	46	4	92
RF defoliation sections	6	22	78.57
Producer's accuracy (%)	88.46	84.62	
Overall accuracy (%) and kappa	87.2	0.717	
		2008	
RF non-defoliation sections	16	9	64
RF defoliation sections	7	29	80.56
Producer's accuracy (%)	69.57	76.32	
Overall accuracy (%) and kappa	73.8	0.451	
		2009	
RF non-defoliation sections	11	11	50
RF defoliation sections	6	53	89.83
Producer's Accuracy (%)	64.71	82.81	
Overall accuracy (%) and kappa	79	0.429	
		2010	
RF non-defoliation sections	13	20	39.39
RF defoliation sections	2	26	92.86
Producer's accuracy (%)	86.67	56.52	
Overall accuracy (%) and kappa	63.9	0.308	

Similar to the results for DI, the error matrix for the ROI-based accuracy assessment suggested little change in pixel-level classification accuracy from 2007 to 2010 (Table 10). 2010 had the highest overall accuracy (86.49%) and kappa coefficient (0.728), while 2009 had the lowest accuracy, with the overall accuracy and kappa coefficient decreasing to 80.57% and 0.609, respectively. Producer's accuracy for non-defoliation was always higher than for defoliation, and user's accuracy for defoliation was always higher than for non-defoliation.

Sensitivity Analysis Results

For both the DI and RF methods, the change in the false positive detection rate corresponding to an increasing threshold of change was examined (Figs. 7 and 8). If

Table 10. RF Error Matrices Showing the Number of Defoliated and Non-defoliated Pixels Classified from ROIs for 2007–2010

	Image-interpreted defoliation pixels	Image-interpreted non-defoliation pixels	User's accuracy (%)
		2007	
RF defoliation pixels	183	12	93.85
RF non-defoliation pixels	88	270	75.42
Producer's accuracy (%)	67.53	95.75	
Overall accuracy (%) and kappa	81.92	0.636	
		2008	
RF defoliation pixels	169	0	100
RF non-defoliation pixels	95	275	74.32
Producer's accuracy (%)	64.02	100	
Overall accuracy (%) and kappa	82.37	0.644	
		2009	
RF defoliation pixels	177	0	100
RF non-defoliation pixels	115	300	72.29
Producer's accuracy (%)	60.62	100	
Overall accuracy (%) and kappa	80.57	0.609	
		2010	
RF defoliation pixels	213	1	99.53
RF non-defoliation pixels	79	299	79.1
Producer's accuracy (%)	72.95	99.67	
Overall accuracy (%) and kappa	86.49	0.728	

the minimum change value was set as the threshold, pixels with values larger than the minimum (all of the pixels) would be classified as positive defoliation detections, so the false positive detection rate would be 100%. If the maximum change value was set as the threshold, pixels with values larger than maximum (none of the pixels) would be classified as defoliated, resulting in a false positive detection rate of 0%, but concurrently no ability to detect defoliation. Figure 7 shows that DI's false positive detection rate decreased near a threshold of zero, but continued to decline at higher threshold values. When exceeding a threshold of 0.2, all the false positive percentages were below 10%. Although the descending trend was similar in all four years, 2009 had the highest false alarm rate at a high DI threshold. Similar to the DI curves in Figure 7, curves for RF showed an overall descending trend as the threshold increased (Fig. 8).

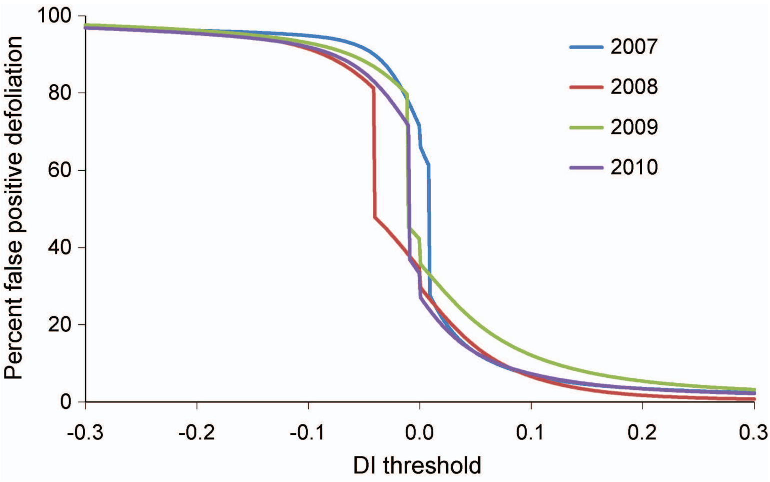

Fig. 7. Change in false positive detection rate with the increasing threshold of DI change.

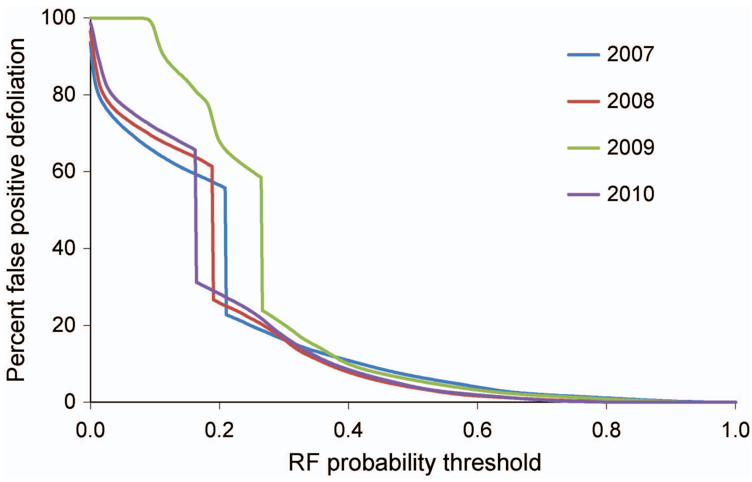

Fig. 8. Change in false positive detection rate with the increasing threshold of RF probability.

In addition, in three years the false positive rate fell rapidly near 0.2 probability threshold. 2007's false alarm rate was the highest after exceeding a threshold of 0.4, while 2008 and 2010 had similar, lower values.

As shown in Figures 9 and Figure 10, increasing the number of pixels required to classify a river section as defoliated generally resulted in changes in kappa values. For the DI method, the overall trend for each year was an increasing kappa, as the number of pixels required in each section was initially increased, followed by a slow decrease in kappa. Changes in kappa were especially large for 2010, for which the kappa value jumped from –0.05 to higher than 0.3 as the number of pixels required for detection reached 10. For the RF method, kappa was highest for one-pixel defoliation detection within each river section, except for 2008.

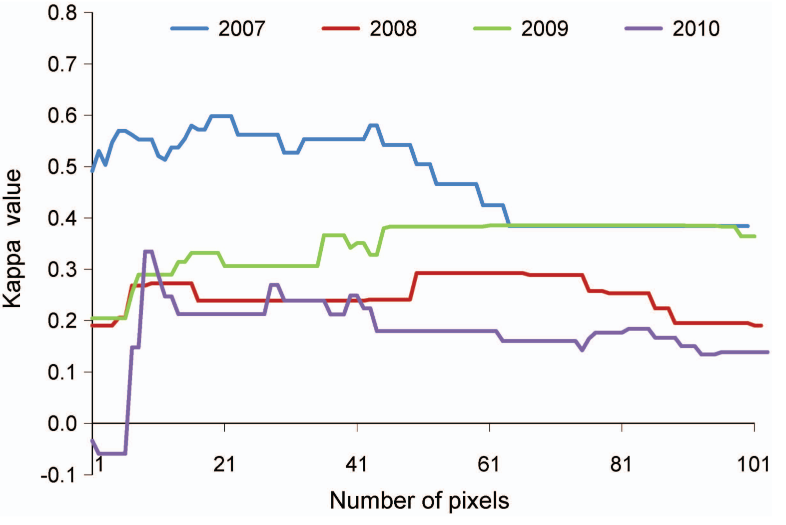

Fig. 9. Change in DI classification kappa value with the increasing number of pixels to classify each river section as a positive detection.

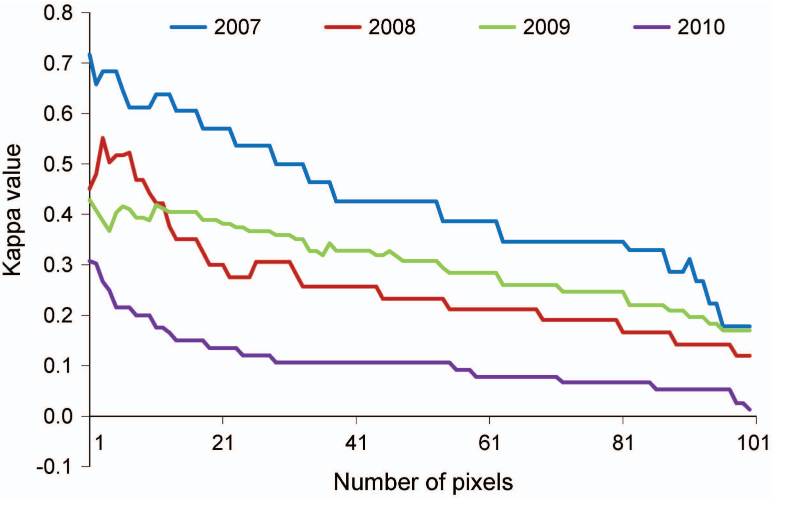

Fig. 10. Change in RF classification kappa value with the increasing number of pixels to classify each river section as a positive defoliation detection.

DISCUSSION

For both the DI and RF methods, defoliation was detected in the middle portion of Colorado River and lower Green River in 2007, which then expanded into the middle portion of the Green River and its tributaries in 2008, and into most of the tributaries in the study area in 2009 and 2010. Each method of classification demonstrated strengths and weaknesses for detection of defoliation, and each method of accuracy assessment demonstrated strengths and weaknesses for verification of defoliation detection. For DI, accuracy assessment based on river sections was overly sensitive to false positive defoliation classifications. A single river section contained hundreds of pixels, and a single pixel within a river section could result in labeling the entire section as defoliated. RF was less sensitive to the number of pixels used to classify a river section as defoliated, however. The ROI-based method evaluated accuracy on a per-pixel level, reducing the impact of false detection of defoliation. Because DI was more prone to false positive detection than RF, the disparities in accuracy between the two accuracy assessment methods were much larger for DI than for RF.

The change detection methods used in this study were based on the assumption that spectral differences indicating changes in canopy cover were directly caused by northern tamarisk beetle herbivory. Tamarisk defoliation by the beetle was the primary disturbance in the study area during the time span covered by this study, and the vast majority of defoliation detections were likely due to actual beetle defoliation. However, other phenomena can also cause a decrease in riparian canopy cover. Manual harvesting, herbicide application, land development, flooding, or varying phenology could also result in changes in canopy cover that could manifest a similar TC signal. Herbivory by another insect, the tamarisk leaf hopper (*Opsius stactogalus*), may have also impacted the classification of defoliation. The leaf hopper can cause yellowing of tamarisk foliage that is pronounced in late August. During field surveys in 2007 and 2008, high leafhopper densities and tamarisk yellowing were observed late in the season.

RF worked as a "black box" classification method and automatically chose the most useful input variables by internal estimation of importance to randomly generate a large ensemble of independent trees for classifying defoliation. RF produced fewer false positive detections of defoliation, which indicates the higher selectivity of this method. However, RF used a much larger set of variables, and relationships between variables were not transparent.

The field survey data were filtered within a time window spanning one week prior to or two weeks following image acquisition. It is possible that a field survey could measure little or no defoliation, and one week later, substantial defoliation could have occurred. On the other hand, an image may measure little or no defoliation and two weeks later a field survey could detect substantial defoliation. The time span used to compare field sampling and remotely sensed data was the result of a tradeoff between the number of field survey points that could be used and the potential accuracy of defoliation mapping. Ideally, all remote sensing and field data would be collected within days of each other.

One method for improving defoliation detection accuracy would be to fine-tune the thresholds used for DI or RF. Making thresholds more selective would reduce defoliation false positives, but would also reduce the number of sections correctly classified as defoliated and reduce the ROI-based accuracy. The subjective choice of an appropriate detection threshold was important for determining the accuracy of detection. The sensitivity analysis showed change in false positive defoliation detection, and the increasing threshold of change in DI or RF probability could help to suggest and choose potential thresholds for both the DI and RF methods. Varying the threshold determined for each image also demonstrated that it may be necessary to assign a threshold independently for each image or for each year. A change in the kappa value with an increasing number of pixels needed to classify a river section as defoliated indicated that the DI method tends to produce more false positive detections and is less selective than the RF method. In future studies, plots indicating the distribution of DI change and RF probability for representative defoliated and non-defoliated pixels should be made for each year to help find appropriate thresholds, instead of manually comparing against an RGB combination of TM bands to find thresholds based on visual inspection. High-quality, representative samples of defoliated and non-defoliated pixels selected across the study area are important for training. In this study, the majority of the training samples were collected from riparian areas along the Green and Colorado rivers. This may explain why RF did a better job detecting defoliated pixels in these two rivers sections, but failed to detect defoliated pixels in narrower tamarisk stands along the San Juan and Dolores rivers.

Another important factor that may have affected accuracy was changes in cloud and shadow cover between images. Pixels contaminated by cloud and cloud shadows could possess large positive DI change values and affect the values of useful input variables of RF. Although cloud and cloud shadows were masked, it is difficult to mask all of the cloud- and shadow-contaminated pixels within a partially cloud covered image. The sensitivity of the DI and RF methods to cloud- and shadow-contaminated pixels may be different: the DI method cannot identify the difference between contaminated and non-contaminated pixels, leading to possible classification of cloud- and shadow-contaminated pixels as defoliated, due to very high brightness, wetness, or very low greenness values of contaminated pixels, which can produce very high DI (Healey et al. 2005). The more complex RF method could be trained to exclude cloud cover as "non-defoliated" land cover. This partially explains why the DI method detected a much larger defoliated area than the RF method for the years (2008–2010) having large cloud and shadow cover.

Spatial resolution is also an important factor affecting the detection of tamarisk defoliation (Dennison et al., 2009). The spatial resolution of TM imagery is 30 meters, and stands of tamarisk in the study area do not typically exceed this areal coverage unless occurring within a major floodplain. Therefore, mixed pixels of tamarisk with other land cover could be common in the study area. These mixtures will reduce spectral changes and make defoliation detection less likely. Very high spatial resolution remote sensing imagery, such as WorldView-2 or GeoEye-1, has the potential ability to monitor defoliation on the scale of individual canopies using other methods, such as object-oriented classification, but would also restrict monitoring over large areas because of difficulties in data acquisition and processing. Shifts in spatial coregistration are another potential factor impacting defoliation detection. Coregistration errors could lead to measurement of defoliation where none exists (Dennison et al., 2009).

CONCLUSIONS

In this study, we assessed the utility of multispectral data for monitoring defoliation of tamarisk by the northern tamarisk beetle as it spread through the study area. We evaluated the accuracy of DI and RF detection methods using field survey data assigned to 10 km river sections and pixel-based image interpretation. Both accuracy assessment methods indicated that the application of DI and RF algorithms to TM imagery may be useful for studying spatiotemporal patterns of tamarisk defoliation. Considering the higher kappa values and reduced false positives for RF, RF is likely to be more useful for monitoring of tamarisk defoliation over time within this specific study area. Since RF is heavily dependent on relationships present in input data, the DI method may be more easily extendable to larger study areas.

Continued investigation of methods for monitoring tamarisk defoliation is still needed, considering the significant impacts of tamarisk and tamarisk defoliation on riparian ecosystems. Higher defoliation detection accuracy may be possible with alternative classification methods, and higher spatial or spectral resolution data may allow separation of defoliation from other types of disturbance that may be falsely detected as defoliation using Landsat TM spatial and spectral resolution. As repeated defoliation can result in tamarisk mortality, methods will need to be developed to use seasonal differences in canopy cover to monitor mortality and successional replacement. Improved remote monitoring of tamarisk defoliation across the western U.S. will assist ongoing management activities designed to protect and sustain highly valued riparian ecosystems throughout the region.

ACKNOWLEDGMENTS

The authors would like to acknowledge the efforts of the Tamarisk Coalition for collecting and compiling the field survey data. The U.S. Geological Survey Southwest Biological Science Center provided financial support for aspects of this study.

REFERENCES

Anderson, G. L., Carruthers, R. I., Ge, S., and P. Gong, 2005, "Monitoring of Invasive Tamarisk Distribution and Effects of Biological Control with Airborne Hyperspectral Remote Sensing," *International Journal of Remote Sensing*, 26(12):2487–2489.

Bailey, J. K., Schweitzer, J. A., and T. G. Whitham, 2001," Salt Cedar Negatively Affects Biodiversity of Aquatic Macroinvertebrates," *Wetlands: The Journal of the Society of the Wetland Scientists,* 21: 442–447.

Banner, A. V. and T. Lynham, 1981,"Multitemporal Analysis of Landsat Data for Forest Cut-over Mapping—a Trial of Two Procedures," in *Proceedings of the 7th Canadian Symposium on Remote Sensing, Canadian Remote Sensing Society*, *Winnipeg, Canada,* 233–240.

Barrows, C. W., 1996, *Tamarisk Control and Common Sense*, San Diego, CA: California Exotic Pest Plant Council.

Blossey, B., 2004, "Monitoring in Weed Biological Control Programs," in *Biological Control of Invasive Plants in the United States*, Coombs, E. M., Clark, J. K., Piper, G. L., and A. F. Cofrancesco (Eds.), Corvallis, OR: Oregon State University Press, 59–105.

Bradley, A. P., 1997, "The Use of the Area under the ROC Curve in the Evaluation of Machine Learning Algorithms," *Pattern Recognition,* 30(7):1145–1159.

Breiman, L., 2001, "Random Forests," *Machine Learning*, 45(1):5–32.

Brown, B., Ruffner, G., Johnson, R., Horton, J., and J. Franson, 1989, *Economic Analysis of Harmful and Beneficial Aspects of Saltcedar*, Mesa, AZ and Boulder City, NV: Great Western Research, Inc., Final Report to USDI Bureau of Reclamation.

Bruzzone, L. and D. F. Prieto, 2000, "Automatic Analysis of the Difference Image for Unsupervised Change Detection," *Geoscience and Remote Sensing. IEEE Transactions on*, 38(3):1171–1182.

Busch, D. E. and S. D. Smith, 1995, "Mechanisms Associated with Decline of Woody Species in Riparian Ecosystems of the Southwestern U.S.," *Ecological Monographs*, 65:347–370.

Carruthers, R. I., DeLoach, C. J., Herr, J. C., Anderson, G. L., and A. E. Knutson, 2008," Salt Cedar Areawide Pest Management in the Western USA," In *Areawide Pest Management: Theory and Implementation,* Koul, O., Cuperus, G., and Elliott, N. (Eds.), Wallingford, UK: CAB International, 271–299.

Canty, M. J. and A. A. Nielsen, 2008, "Automatic Radiometric Normalization of Multitemporal Satellite Imagery with the Iteratively Re-weighted MAD Transformation," *Remote Sensing of Environment,* 112: 1025–1036.

Cleverly, J. R., Smith, S. D., Sala, A., and D. A. Devitt, 1997, "Invasive Capacity of *Tamarix ramosissima* in a Mojave Desert Floodplain: The Role of Drought," *Oecologia*, 111:12–18.

Cohen, J. A., 1960, "A Coefficient of Agreement for Nominal Scales," *Educational and Psychological Measurement,* 20:37–46.

Coops, N. C., Johnson, M., Wulder, M. A., and J. C. White, 2006, "Assessment of QuickBird High Spatial Resolution Imagery to Detect Red Attack Damage Due to Mountain Pine Beetle Infestation," *Remote Sensing of Environment*, 103(1):67–80.

Coppin, P. R. and M. E. Bauer, 1996, "Change Detection in Forest Ecosystems with Remote Sensing Digital Imagery," *Remote Sensing Reviews*, 13:207–234.

Crist, E. P. and R. C. Cicone, 1984, "A Physically-Based Transformation of Thematic Mapper Data—the TM Tasseled Cap," *IEEE Transactions on Geoscience and Remote Sensing*, 22(3):256–263.

DeLoach, C. J., Lewis, P. A., Herr, J. C., Carruthers, R. I., Tracy, J. L., and J. Johnson, 2003, "Host Specificity of the Leaf Beetle, *Diorhabda elongata deserticola* (Coleoptera: Chrysomelidae) from Asia, a Biological Control Agent for Saltcedars (*Tamarix*: Tamaricaceae) in the Western United States," *Biological Control*, 27(2):117–147.

DeRose, R. J., Long, J. N., and R. D. Ramsey, 2011, "Combining Dendrochronological Data and the Disturbance Index to Assess Engelmann Spruce Mortality Caused by a Spruce Beetle Outbreak in Southern Utah, USA," *Remote Sensing of Environment* , 115:2342–2349.

Dennison, P. E., Nagler, P. L., Hultine, K. R., Glenn, E. P., and J. R. Ehleringer, 2009, "Remote Monitoring of Tamarisk Defoliation and Evapotranspiration Following Saltcedar Leaf Beetle Attack," *Remote Sensing of Environment*, 113:1462–1472.

Dudley, T. L. and D. W. Bean, 2012, "Tamarisk Biocontrol, Endangered Species Risk and Resolution of Conflict through Riparian Restoration," *Biological Control*, 57:331–347.

Dudley, T. L., DeLoach, C. J., Lovich, J., and R. I. Carruthers., 2000, "Saltcedar Invasion of Western Riparian Areas: Impacts and New Prospects for Control," in

Transactions of the 65th North American Wildlife & Nature Resource Conference, March 2000, Chicago, 345–381.

Friedman, J. T., Auble, G. T., Shafroth, P. B., Scott, M. L., Merigliano, M. F., Freehling, M. D., and E. R. Griffin, 2005, "Dominance of Non-native Riparian Trees in Western USA," *Biological Invasions*, 5:747–751.

Hais, M., Jonášová, M., Langhammer, J., and T. Kučera , 2009, "Comparison of Two Types of Forest Disturbance Using Multitemporal Landsat TM/ETM+ Imagery and Field Vegetation Data," *Remote Sensing of Environment*, 113(4):835–845.

Harms, R. S. and R. D. Hiebert, 2006, "Vegetation Response Following Invasive Tamarisk (*Tamarix* spp.) Removal and Implications for Riparian Restoration," *Restoration Ecology*, 14(3):461–472.

Healey, S. P., Cohen, W. B., Zhiqiang, Y., and O. N. Krankina, 2005, "Comparison of Tasseled Cap–Based Landsat Data Structures for Use in Forest Disturbance Detection," *Remote Sensing of Environment*, 97(3):301–310.

Howarth, P. J. and G. M. Wickware, 1981, "Procedures for Change Detection Using Landsat Digital Data," *International Journal of Remote Sensing*, 2(3):277–291.

Hultine, K. R., Belnap, J., van Riper III, C., Ehleringer, J. R., Dennison, P. E., Lee, M. E., Nagler, P. L., Snyder, K. A., Uselman, S. M., and J. B. West, 2010a, "Tamarisk Biocontrol in the Western United states: Ecological and Societal Implications," *Frontiers in Ecology and the Environment*, 8(9):467–474.

Hultine, K. R., Nagler, P. L., Dennison, P. E., Bush, S. E., and J. R. Ehleringer, 2009, "Tamarisk (*Tamarix* spp.) Water Fluxes before, during, and after Episodic Defoliation by the Saltcedar Leaf Beetle," *Acta Horticulturae*, 846:293–302.

Hultine, K. R., Nagler, P. L., Morino, K., Bush, S. E., Burtch, K. G., Dennison, P. E., Glenn, E. P., and J. R. Ehleringer ,2010b, "Sap Flux-scaled Transpiration by Tamarisk (*Tamarix* Spp.) before, during, and after Episodic Defoliation by the Saltcedar Leaf Beetle (*Diorhabda* carinulata)," *Agricultural and Forest Meteorology*, 150(11):1467–1475.

Hurley, A., Watts, D., Burke, B., and C. Richards, 2004, "Identifying Gypsy Moth Defoliation in Ohio Using Landsat Data," *Environmental Engineering Geoscience*, 10(4):321–328.

Jackson, R. D., 1986, "Remote Sensing of Biotic and Abiotic Plant Stress," *Annual Review of Phytopathology*, 24:265–287.

Jin, S. and S. A. Sader, 2005, "Comparison of Time Series Tasseled Cap Wetness and the Normalized Difference Moisture Index in Detecting Forest Disturbances," *Remote Sensing of Environment*, 94(3):364–372.

Johns, E. L., 1989, *Water Use by Naturally Occurring Vegetation, Including an Annotated Bibliography*, New York, NY: American Society of Civil Engineers.

Joshi, C., Leeuw, J. D., and I. C. V. Duren, 2004, "Remote Sensing and GIS Applications for Mapping and Spatial Modeling of Invasive Species," in *XXth ISPRS Congress. Commission 7, Istanbul, Turkey*, 669–678.

Kennedy, R. E., Yang, Z., and W. B. Cohen, 2010, "Detecting Trends in Forest Disturbance and Recovery Using Yearly Landsat Time Series: 1. LandTrendr—Temporal Segmentation Algorithms," *Remote Sensing of Environment,* 114:2897–910.

Kharuk, V. I., Ranson, K. J., Kuz'michev, V. V., and S. T. Im, 2003, "Landsat-Based Analysis of Insect Outbreaks in Southern Siberia," *Canadian Journal of Remote Sensing*, 29(2): 286–297.

Lesica, P. and S. Miles, 2004, "Ecological Strategies for Managing Tamarisk on the C. M. Russell National Wildlife Refuge, Montana, USA," *Biological Conservation*, 119:535–543.

Lewis, P. A., DeLoach, C. J., Knutson, A. E., Tracy, J. L., and T. O. Robbins, 2003, "Biology of *Diorhabda elongata deserticola* (Coleoptera: Chrysomelidae), an Asian Leaf Beetle for Biological Control of Saltcedars (*Tamarix* spp.) in the United States," *Biological Control*, 27(2):101–116.

Liaw, A. and M. Wiener, 2002, "Classification and Regression by Random Forest," *R News,* 2(3):18–22.

Lodwick, G. D., 1979, "Measuring Ecological Changes in Multitemporal Landsat Data Using Principal Components," in *Proceedings of the 13th International Symposium on Remote Sensing of Environment*, *Environmental Research Institute of Michigan, Ann Arbor, Michigan*, 1–11.

Malila, W. A., 1980, "Change Vector Analysis: An Approach for Detecting Forest Changes with Landsat," in *Machine Processing of Remotely Sensed Data Symposium, IEEE*, 326–335.

Moran, P. J., DeLoach, C. J., Dudley, T. L., and J. Sanabria , 2009, "Open Field Host Selection and Behavior by Tamarisk Beetles (*Diorhabda* spp.) (Coleoptera: Chrysomelidae) in Biological Control of Exotic Saltcedars (*Tamarix* spp.) and Risks to Non-target Athel (*T. aphylla*) and Native *Frankenia* spp.," *Biological Control*, 50:243–261.

Nilsson, H., 1995, "Remote Sensing and Image Analysis in Plant Pathology," *Annual Review of Phytopathology*, 33:489–528.

Pal, M. and P. M. Mather, 2003, "An Assessment of the Effectiveness of Decision Tree Methods for Land Cover Classification," *Remote Sensing of Environment*, 86:554–565.

Pattison, R. R., D'Antonio, C. M., and T. L. Dudley, 2011, "Biological Control Reduces Growth, and Alters Water Relations of the Saltcedar tree (*Tamarix* spp.) in Western Nevada, USA," *Journal of Arid Environments*, 75(4):346–352.

Shafroth, P. B., Cleverly, J., Dudley, T. L., Stuart, J., Van Riper III, C., and E. P. Weeks, 2005, "Saltcedar Removal, Water Salvage and Wildlife Habitat Restoration along Rivers in the Southwestern U.S.," *Environmental Management*, 35:231–246.

Singh, A., 1989, "Review Article: Digital Change Detection Techniques Using Remotely-Sensed Data," *International Journal of Remote Sensing*, 10(6):989–1003.

Skakun, R. S., Wulder, M. A., and S. E. Franklin, 2003, "Sensitivity of the Thematic Mapper Enhanced Wetness Difference Index to Detect Mountain Pine Beetle Red-Attack Damage," *Remote Sensing of Environment*, 86(4):433–443.

Smith, A. M. S., Wooster, M. J., Powell, A. K., and D. Usher, 2002, "Texture Based Feature Extraction: Application to Burn Scar Detection in Earth Observation Satellite Sensor Imagery," *International Journal of Remote Sensing,* 23:1733–39.

Tracy, J. T. and T. O. Robbins, 2009, "Taxonomic Revision and Biogeography of the *Tamarix*-Feeding *Diorhabda elongata* (Brullé, 1832) Species Group (Coleoptera: Chrysomelidae: Galerucinae: Galerucini) and Analysis of Their Potential in Biological Control of Tamarisk," *Zootaxa*, 2101:1–152 van Riper III, C., Paxton, K. L., O'Brien, C., Shafroth, P. B., and L. J. McGrath, 2008, "Rethinking Avian Response to Tamarisk on the Lower Colorado River: A Threshold Hypothesis," *Restoration Ecology,* 16:152–164.

Wang, F., 1993, "A Knowledge-Based Vision System for Detecting Land Changes at Urban Fringes," *IEEE Transactions on Geoscience and Remote Sensing*, 31(1):136–145.

Warren, D. K. and R. M. Turner, 1975, "Saltcedar (*Tamarix chinensis*) Seed Production, Seedling Establishment, and Response to Inundation," *Journal of the Arizona Academy of Science*, 10:135–144.

Weismiller, A., Kristofs, J., Schlzd, K., Anutap, E., and A. Momens, 1977, "Change Detection in Coastal Zone Environments," *Photogrammetric Engineering and Remote Sensing and Digital Image Processing,* 43:1533–1539.

Wilson, J. R., Blackman, C., and G. W. Spann, 1976, "Land Use Change Detection Using Landsat Data," in *Proceedings of the 5th Annual Remote Sensing for Earth Resources Conference*. *University of Tennessee, Tullahama, TN*, 79–91.

Zavaleta, E., 2000, "The Economic Value of Controlling an Invasive Shrub," *Ambio*, 29:462–467.